of field errors. From Eq. (4) it can be seen that large τ_b/τ_r requires large p (i.e., short-wavelength errors), in order that the Maxwellian particle distribution be nonzero at the resonant velocity. The data for small τ_b/τ_r are more readily explained by small-p errors, since the theoretical model is suspect at extremely low particle energies. No unifying relation between the two parameter regimes is as yet apparent, and it is surprising that the data scale so regularly over the range in τ_b/τ_r.

We have experimentally verified that azimuthally asymmetric voltages applied to the wall sectors induce radial transport.[14] This transport generally increases with increasing plasma length, and decreases with increasing magnetic field. Magnetostatic perturbations also induce transport, but are less easily manipulated experimentally. We are presently attempting to relate quantitatively the induced transport to the predictions of theory. Correspondence with the naturally occurring transport has not yet been established.

In summary, we have observed pressure-independent particle transport rates scaling as L^2/B^2 over more than five decades. We believe that this transport is caused by small azimuthal asymmetries in the applied magnetic or electric fields. The data are reasonably compatible with single-particle resonant transport theory, but other processes are by no means excluded.

We wish to thank Professor T. M. O'Neil for many useful discussions. This work is based on research supported by the National Science Foundation under Grant No. PHY80-09326.

[1]R. C. Davidson, *Theory of Nonneutral Plasmas* (Benjamin, Reading, Mass., 1974).
[2]J. H. Malmberg and J. S. deGrassie, Phys. Rev. Lett. 35, 577 (1975).
[3]T. M. O'Neil, Phys. Fluids 23, 2216 (1980).
[4]M. H. Douglas and T. M. O'Neil, Phys. Fluids 21, 920 (1978).
[5]J. S. deGrassie and J. H. Malmberg, Phys. Fluids 23, 63 (1980).
[6]J. H. Malmberg and C. F. Driscoll, Phys. Rev. Lett. 44, 654 (1980).
[7]Length-dependent transport has also been observed on a second electron-plasma apparatus. This apparatus operates at liquid helium temperatures, has a superconducting coil with 4×10^4 turns, and has no magnetic materials in the containment device.
[8]R. H. Cohen, Comments Plasma Phys. Controlled Fusion 4, 157 (1978).
[9]D. D. Ryutov and G. V. Stupakov, Dok. Akad. Nauk SSSR 240, 1086 (1978) [Sov. Phys. Dokl. 23, 412 (1978)].
[10]M. E. Kishinevskij *et al.*, in *Proceedings of the Seventh International Conference on Plasma Physics and Controlled Nuclear Fusion Research, Innsbruck, Austria, 1978* (International Atomic Energy Agency, Vienna, Austria, 1979), Vol. 2, p. 411.
[11]T. M. O'Neil, Phys. Fluids 23, 725 (1980).
[12]R. J. Briggs, J. D. Daugherty, and R. H. Levy, Phys. Fluids 13, 421 (1970).
[13]W. D. White, J. H. Malmberg, and C. F. Driscoll, Bull. Am. Phys. Soc. 26, 855 (1981).
[14]D. L. Eggleston and J. H. Malmberg, Bull. Am. Phys. Soc. 27, 1031 (1982).

Measurements of the Effect of Tokamak Magnetic Field Helicity on Lower Hybrid Resonance Cones

P. M. Bellan
California Institute of Technology, Pasadena, California 91125
(Received 29 November 1982)

The effect of tokamak magnetic field helicity, i.e., rotational transform, on the propagation of lower hybrid resonance cones is clearly observed in the California Institute of Technology Encore tokamak. The observations are in excellent agreement with the predictions of a recent theory.

PACS numbers: 52.35.Fp, 52.40.Fd

Lower hybrid waves are under active investigation as a possible means for driving steady-state dc currents in tokamaks and also for heating tokamak plasmas to fusion ignition. The fundamental behavior of lower hybrid propagation in *straight* magnetic field geometry has been well established; in particular, it has been shown that lower hybrid waves propagate as *resonance cones*[1-3] (described by the cold-plasma, electrostatic two-fluid equations) and that these cones have a fine structure dictated by the geometry of the exciting antenna[4] and also by higher-order

thermal[1] and electromagnetic[5] effects.

Tokamaks have *helical*, rather than straight, magnetic field lines so that the geometry of propagation will be different from that of Refs. 1–3. Plane-ray-tracing calculations for tokamak geometry by Ejima *et al.*[6] and Bonoli and Ott[7] have given valuable insight into the effect of magnetic field helicity, but these calculations do not take into account the resonance-cone nature of the propagation. The author recently presented[8] an analytic and numerical calculation which does take this resonance-cone nature into account, and so gives a more realistic picture of the geometry of the wave propagation. In this Letter I present the first experimental measurements of the effect of tokamak magnetic field helicity (i.e., rotational transform) on lower hybrid resonance cones, and show that these measurements are in excellent agreement with the predictions of Ref. 8.

The experiments were performed on the California Institute of Technology Encore tokamak (major radius 38 cm, minor radius 12 cm). Because of Encore's extremely high (15 shots/sec) repetition rate and modest plasma parameters [$n \sim (0.3\text{–}2) \times 10^{12}$ cm^{-3}, $B_\varphi \sim 0.5\text{–}1.6$ kG, $I_p \sim 0.5\text{–}8$ kA, $T_e \sim 4\text{–}15$ eV, Ar gas, shot duration 2 msec] it was possible to track the cone propagation with an rf probe.

Figure 1 shows the experimental setup. Six dipole transmitting antennas are located in the midplane at the outer edge of the plasma. These antennas are separated 18, 36, 54, 90, 108, and 126 toroidal degrees from an rf receiving probe which can be moved both horizontally and vertically (i.e., in R and z, respectively) by computer controlled stepping motors. The transmitting probes are dipoles so as to avoid exciting a long-wavelength cavity mode in the tokamak. To further suppress measurement of any remnants of this mode the receiving probe is double tipped

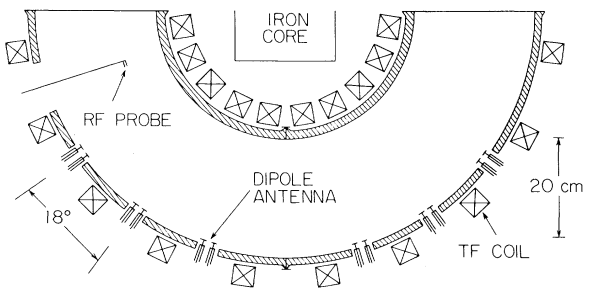

FIG. 1. Experimental setup. Receiving probe moves in two dimensions: major radius R and vertical position z (here, z is into or out of page).

(1-mm spacing between 5-mm-long tips), and the difference signal is measured by using a 180° power combiner. It was found that, because of slight asymmetries in the cabling, the signal amplitudes from the two tips were not exactly equal. To compensate for this, two electronically adjustable rf attenuators (one for each probe tip) were used to equalize the signal levels, and so obtain optimum common-mode rejection when the signals are subtracted in the power combiner.

A DEC LSI-11/23 computer controls the receiving-probe horizontal and vertical positioning, processes the data, displays the results on a graphics CRT monitor, and compares (also on the graphics monitor) these results with the theory of Ref. 8. In a typical measurement the receiving probe is scanned horizontally (in 246 steps) at a sequence of vertical positions so as to make a raster scan of the tokamak minor cross section. A fast (25-μsec switching time) Lorch Electronics multipole rf switch, sequenced by an external clock, is used to time multiplex a 15-dBm 450-MHz rf signal to six 500-mW rf amplifiers. Each amplifier is connected through an rf dc-isolation transformer to one of the six respective transmitting antennas. Thus, at each position in its scan of the minor cross section, the rf probe measures (in rapid sequence) the signals emitted by all six transmitters. The rf probe signal is fed into either an amplitude detector or an rf interferometer depending on whether amplitude or phase information is desired. The output of these instruments goes to a Transiac 2008 CAMAC transient digitizer, also cycled by the clock which sequences the rf switch. The transient digitizer memory is passed to the computer, which thus distinguishes antennas according to memory location in the digitizer. Hence, with this system, minor-cross-section scans at six different transmitter-receiver toroidal separations are made essentially simultaneously, giving in effect a three-dimensional picture of the wave propagation. The six minor-cross-section scans are plotted on a 512×512 pixel graphics monitor, the display of which can be transferred to a dot matrix printer.

Successful interferometer scans, i.e., those for which the wave phase was observable, could only be made when the density and magnetic fluctuation levels were low. Low fluctuation levels were achievable over only a limited range of plasma parameters, generally those having high q and a very specific setting of the equilibrium vertical field; otherwise there were substantial den-

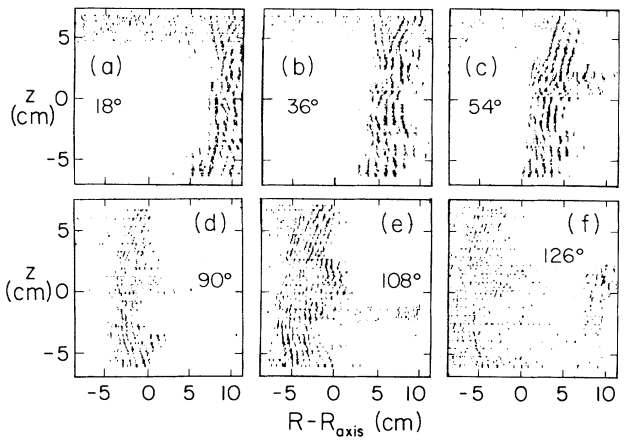

FIG. 2. Interferometry, tokamak adjusted for low fluctuation level. (a)–(f): Phase fronts over the minor cross section for the six respective transmitter antennas; amplitude information has been suppressed by the computer. $f = 450$ MHz, $I_p = 700$, A, $B_\varphi = 690$ G, $q_{wall} = 20$, filling pressure = 5×10^{-5} Ar.

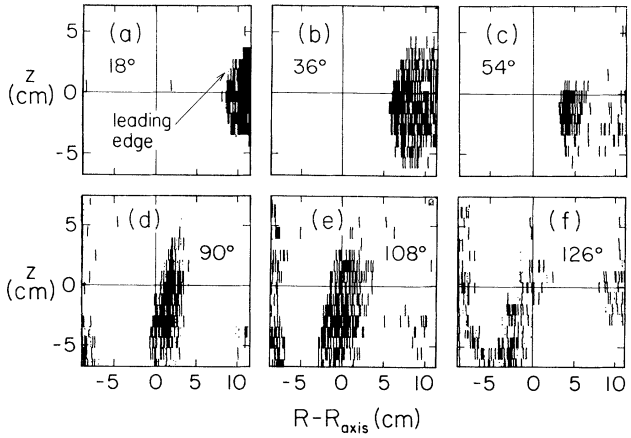

FIG. 3. Wave amplitude for the six transmitters. $f = 450$ MHz, $I_p = 2600$ A, $B_\varphi = 1035$ G, $n = 10^{12}$ cm^{-3}, $q_{wall} = -8$, filling pressure = 2×10^{-5} Ar. Loci of leading edges [cf. (a)] for different values are plotted in Fig. 4.

sity and magnetic fluctuations, in which case the interferometer signal phase mixed to zero. Figures 2(a)–2(f) show a set of minor-cross-section phase-front measurements obtained by interferometry in a quiet, high-q plasma. The cone nature of propagation and the fine-structure wiggles due to the electromagnetic interference pattern are clearly visible. It should be pointed out that Fig. 2 indicates phase only; all amplitude information has been suppressed by the computer. Separate amplitude measurements indicate that the amplitude at the midplane exceeds the amplitude at the top and bottom by factors of 5–10, so that the complicated structures at the top and bottom are relatively unimportant.

Figures 3(a)–3(f) show measurements of the cone amplitude (measured by a square-law amplitude detector) in a situation where the plasma is too noisy for interferometry. Here, dark areas indicate regions in the minor cross section where the amplitude is greater than 0.2× the maximum amplitude for the respective transmitter. The signals at the far left side of Figs. 3(d)–3(f) are believed to be cones coming the long way around the torus from the antenna.

Additional amplitude measurements, not shown here for lack of space, indicate that fluctuations spread out the signals, but significantly the spreading is mainly in the direction of reduced penetration into the plasma (i.e., to the right side in Fig. 3). This is because fluctuations mainly scatter the cone rays in the poloidal direction, resulting in a reduced radial penetration for a given axial displacement. In effect, the quiet-cold-plasma electrostatic resonance cone gives the maximum radial penetration into the plasma of the actual waves.

Figure 4, the main result presented here, shows the leading edge of measured cone amplitudes [corresponding to the far left side of the amplitude plots, as shown in Fig. 3(a)] for four different values of q ($=RB_\theta/rB_\varphi$) at the wall, having both positive and negative values. The change of sign of q_{wall} was obtained by reversing the direction of B_φ. The successive locations of the cold-plasma resonance cone calculated by using the theory of Ref. 8 are shown as solid lines in Fig. 4. It is clearly seen that the cone is shifted above ($+veq_{wall}$) or below ($-veq_{wall}$) the midplane in roughly inverse proportion to $|q_{wall}|$ and that there is excellent agreement between the experimental measurements and the predictions of the theory of Ref. 8. Hence, as predicted in Ref. 8, the effect of magnetic field helicity is to contort the cone so that the cone axis follows the field helicity.

The Langmuir-probe density measurements made here have about a factor of 2 uncertainty; however, because $\omega_{pe} \gg \omega_{ce}$ for the parameters of this experiment, this uncertainty is not important because the cone angle θ_c is $\theta_c \approx \omega/\omega_{ce}$, and so is essentially independent of density (theory curves at 2× and 5× the densities used here lie nearly on top of the curves of Fig. 4). For the

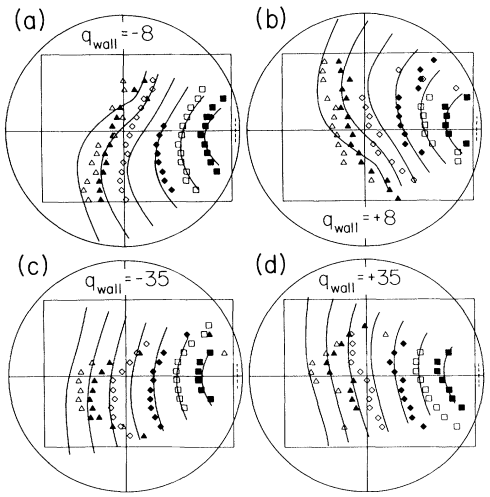

FIG. 4. Leading edge [as in Fig. 3(a)] of wave amplitude for four values q_{wall} compared with theory of Ref. 8; $f = 450$ MHz, $B_\varphi = 1035$ G. Toroidal separation between receiving probe and transmitter probe is indicated as follows: solid squares, 18°; open squares, 36°; solid diamonds, 54°; open diamonds, 90°; solid triangles, 108°; open triangles, 126°. (a) Same data as Fig. 3; (b) same as (a) except direction of B_φ is reversed; (c) $q_{wall} = -35$, $I_p = 600$ A, filling pressure $= 5\times10^{-5}$, $n = 3\times10^{11}$ cm^{-3}; (d) same as (c) except direction of B_φ is reversed. Solid lines are predictions of theory for 18° successive antenna-receiver separations, large rectangle indicates area traversed by receiving probe, large circle indicates 12-cm-radius minor cross section of Encore, while dashed line at right side indicates antenna location.

theoretical curves in Fig. 4 the density n and toroidal field B_φ are related to their values at the magnetic axis by

$$n(r) = n_{axis}[1 - (r/a)^2].$$

$$B_\varphi(r,\theta) = B_{\varphi axis}/[1 + (r\cos\theta)/R_{axis}],$$

where a is the machine minor radius, r is the local minor radius, θ is the poloidal angle, and R is the major radius. The safety factor q is given by the standard parametrization[9]

$$q(r) = q_{axis}[1 + (r/r_0)^4]^{1/2},$$

where r_0, the measure of the current channel width (typically about half the minor radius), has been chosen to be 5 cm. q_{axis} is adjusted so that $q(r_{wall})$ agrees with the measured value.

In Ref. 8 it is also shown that finite-poloidal-extent sources excite fields that poloidally converge, i.e., focus, while point sources excite fields which poloidally diverge. When the plasma is quiet there is evidence of such poloidal focusing due to the finite poloidal extent of the 2.5-cm-high antennas [dashed lines in Figs. 4(a)–4(d)]. For example, Figs. 4(c) and 4(d) show evidence of the cone being concentrated into a smaller poloidal extent than the theoretical curve, which is based on the assumption of a point antenna. When the plasma is noisy [e.g., Figs. 4(a) and 4(b)], the cone is scattered poloidally by fluctuations so that the poloidal focusing becomes smeared out.

From these results the following picture emerges for the propagation of lower hybrid waves excited by a grill antenna in a large tokamak (e.g., Alcator-C, PLT, etc.): The grill excites a field pattern determined by the phasing of the grill elements and also by a combination of the thermal and electromagnetic interference effects. The envelope of this field pattern follows a resonance-cone trajectory and the cone axis follows the local magnetic field helicity. Because the poloidal extent of the grill is typically large (i.e., much greater than typical perpendicular wavelengths), there will be poloidal focusing of the field as it propagates into the plasma. However, fluctuations will poloidally scatter this focused field; thus, the time-averaged field will be smeared out poloidally. The leading edge of the smeared field will simply be the cold-plasma electrostatic resonance-cone trajectory.

The author wishes to thank F. T. Cosso for assistance with the electronics and E. D. Fredrickson for assistance with the Langmuir probe. This work has been supported by National Science Foundation Grant No. ECS-8113533.

[1]R. K. Fisher and R. W. Gould, Phys. Rev. Lett. 22, 1093 (1969), and Phys. Fluids 14, 857 (1971).
[2]H. H. Kuehl, Phys. Fluids 16, 1311 (1973).
[3]R. J. Briggs and R. R. Parker, Phys. Rev. Lett. 29, 852 (1972).
[4]P. Bellan and M. Porkolab, Phys. Rev. Lett. 34, 124 (1975), and Phys. Fluids 17, 1592 (1974).
[5]P. M. Bellan, Phys. Rev. Lett. 45, 1407 (1980).
[6]S. Ejima, V. S. Chan, R. La Haye, C. Moeller, P. I. Petersen, and J. C. Wesley, Bull. Am. Phys. Soc. 22, 1170 (1977).
[7]P. T. Bonoli and E. Ott, Phys. Fluids 25, 359 (1982).
[8]P. M. Bellan, to be published.
[9]B. Carreras, B. V. Waddell, and H. R. Hicks, Nucl. Fusion 19, 1423 (1979).